

UC Davis

UC Davis Previously Published Works

Title

Exposure time dependence of image quality in high-speed retinal in vivo Fourier domain OCT

Permalink

<https://escholarship.org/uc/item/1q21b8jw>

Authors

Zawadzki, Robert J
Bower, Bradley A
Zhao, Mingtao
[et al.](#)

Publication Date

2005-04-18

DOI

10.1117/12.591660

Peer reviewed

Exposure time dependence of image quality in high-speed retinal *in vivo* Fourier-domain OCT

Robert J. Zawadzki^{a*}, Bradley A. Bower^b, Mingtao Zhao^b, Marinko Sarunic^b, Sophie Laut^a
John S. Werner^a and Joseph A. Izatt^b

^a Department of Ophthalmology and Visual Science, UC Davis, 4860 Y Street, Suite 2400,
Sacramento, CA 95817

^b Department of Biomedical Engineering, Duke University, 101 Science Drive, Durham, NC 27708

ABSTRACT

We built a Fourier domain optical coherence tomography (FD-OCT) system using a line scan CCD camera that allows real time data display and acquisition. This instrument is able to produce 2D B-scans as well as 3D data sets with human subjects *in vivo* in clinical settings. In this paper we analyze the influence of varying exposure times of the CCD detector on image quality. Sensitivity values derived from theoretical predictions have been compared with measurements (obtained with mirrors and neutral density filters placed in both interferometer arms). The results of these experiments, discussion about differences between sensitivity values, potential sources of discrepancies, and recommendations for optimal exposure times will be described in this paper. A short discussion of observed artifacts as well as possible ways to remove them is presented. The influence of relative retinal position with respect to reference mirror position will also be described.

Keywords: optical coherence tomography, imaging systems, medical and biomedical imaging, digital image processing, ophthalmology

1. INTRODUCTION

Fourier Domain OCT (FD-OCT) [1,2] has, in recent years, substantially improved relative to standard time-domain OCT [3]. Until recently, however, only the Spectral OCT, the variation of FD-OCT that uses a spectrometer to record tomographic data, has shown its full power for *in vivo* retinal imaging [4-6] and has been extended toward ultrahigh resolution imaging [7-9]. The main benefits of Fourier-domain as compared to time-domain OCT arises from two facts. First, with FD-OCT depth information is acquired in parallel without the requirement of reference arm scanning. Second, FD-OCT offers the possibility of real-time and ultrahigh-resolution imaging. The latter possibility results from the sensitivity advantage of FD-OCT compared to time-domain OCT, and absence of the dependence of the light source bandwidth on sensitivity [10-12].

In this paper, we focus on exposure time as an important design parameter for Spectral OCT systems used for retinal imaging. As in conventional OCT, increasing exposure time increases the theoretical image signal-to-noise ratio. However, decreased image quality can arise *in vivo* due to increased motion artifact susceptibility of Fourier-domain OCT systems [13]. In addition, the coherence noise terms may become prominent for longer exposure times. To explore this trade-off, we obtained high-speed *in vivo* retinal images from healthy human volunteers for different exposure times (from 50 μ s to 5 ms per A-scan, 1000 A-scans/image).

*rjzawadzki@ucdavis.edu; phone (916) 734-5839; fax (916) 734-4543

2. MATERIALS AND METHODS

To describe the effects that reduce *in vivo* FD-OCT image quality, some commonly used equations and concepts will be reviewed.

2.1 Theory

Following Nassif et. al. [6], the Spectral OCT signal measured by the spectrometer can be described as:

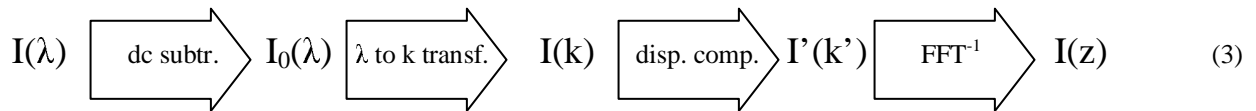
$$I(k) = I_r(k) + I_s(k) + 2\sqrt{I_r(k)I_s(k)} \sum_n \alpha_n \cos(kz_n) \quad (1)$$

where, $I_r(k)$, $I_s(k)$ are wavelength-dependent intensities from reference and sample arm, respectively; k refers to wave number and α_n is a square root of sample reflectivity at depth z_n . The depth information (equivalent to a time-domain OCT A-scan signal) can be accessed by the inverse Fourier transform of Spectral data seen in Eq. 1:

$$I(z) = \left| FT^{-1}[I(k)] \right|^2 = \Gamma^2(z) \otimes \left\{ \delta(0) + \sum_n \alpha_n^2 \delta(z \pm z_n) + O[I_s^2/I_r^2] \right\} \quad (2)$$

where, $\Gamma(z)$ is the envelope of the light source coherence function, also acting as axial point spread function of OCT system, is convolved (\otimes) with OCT signal, being represented by a sum of all reflecting structures at depth z_n , as well as with autocorrelation $\delta(0)$ and coherence noise $O[I_s^2/I_r^2]$ terms.

In order to acquire artifact-free images, several image processing steps including DC subtraction (for autocorrelation and some of coherent noise removal), and λ to k transformation (spectrometer measures $I(\lambda)$) must be performed. The use of software dispersion compensation methods described by Wojtkowski et al [8], interpolation and zero padding plays an important role too. These steps can be summarized by the following representation:



where $I(z)$ is the A-scan intensity of the sample object as a function of depth. As can be seen from Eq. 2, signal value at depth z is directly connected with sample reflectivity α_n at this depth.

There are theoretical models allowing prediction of signal-to-noise ratio (SNR) for known objects. In the case of shot noise-limited detection, the SNR for a given sample arm power P_{sample} returning from the scattering structure placed in the detection arm is given by:

$$SNR_{FD} = \frac{\eta P_{\text{sample}} \tau_i}{E_v} \quad (4)$$

where η is spectrometer efficiency, τ_i is detector integration time and E_v is photon energy.

Even more useful quantities describing performance of any OCT system is its sensitivity (Σ) derived from SNR values. It is defined as an inverse of the object's minimum reflectivity that will produce an OCT signal barely visible on the image (for SNR equal to unity) [14].

$$\Sigma = \frac{1}{R_{s,\min}} \Big|_{SNR=1} \quad (5)$$

Thus, by knowing all parameters in Eq. 4. one can predict FD-OCT system sensitivity. Experimental results show that sensitivity of at least 90 dB is necessary for good quality retinal imaging.

One method for measuring system sensitivity is to place a known neutral density filter (NDF) into the sample arm (with a mirror in the plane of the eye) and then to measure SNR. Sensitivity can be calculated as:

$$\Sigma = 20NDF + 20\log(SNR) \quad (6)$$

where noise value is measured as the standard deviation of the signal. We will use this method to estimate our system performance.

One should remember that sensitivity as well as SNR in FD-OCT decreases with the distance from the reference position (zero path length difference). In Spectral OCT this decay arises from aberrations in the imaging spectrometer and from the finite size of the CCD detector pixel. Thus, the signal seen by the CCD may be described as follows:

$$I_{spectr}(k) = R(k) \otimes I(k) \quad (7)$$

where I_{spectr} represents the measured Spectral signal and $R(k)$ is the total resolving power of the spectrometer (including CCD sampling, diffraction limited spot and diffraction grating resolving power). Thus, following the Fourier Transform, the decay of the signal can be described as the Fourier transform of total resolving power of spectrometer having Sincus like shape [10]:

$$I_{real}(z) = I(z) FT^{-1}[R(k)] \quad (8)$$

Other factors that can decrease the image quality are the possible sample axial and transverse motions. This case has been already extensively described by Yun et al.[13].

2.2 Experimental

The FD-OCT system used for experiments presented in this paper is illustrated in Fig. 1.

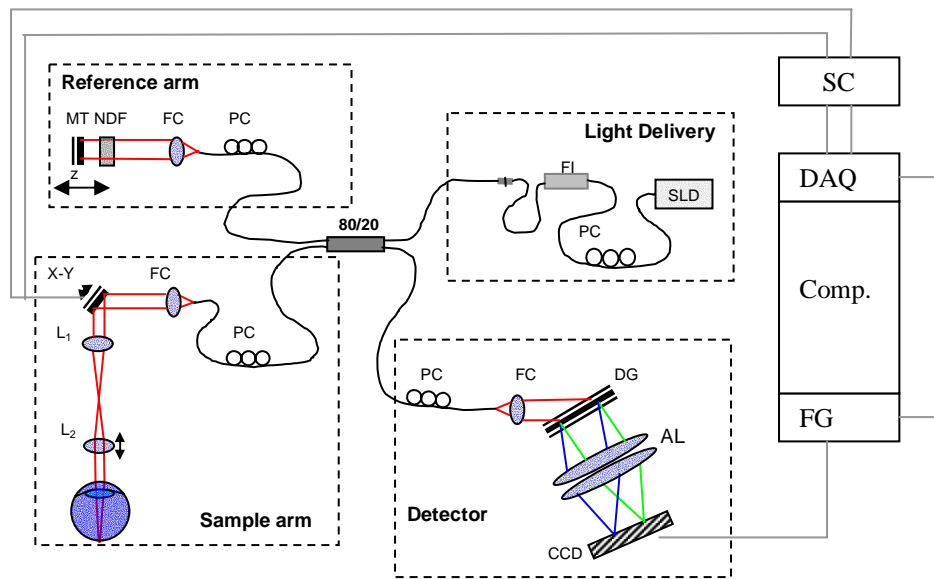


Figure 1: Schematic of experimental setup. The black lines represent optical paths and grey lines represent electronic paths. 80/20 – fiber coupler, Comp. – personal computer, DAQ – data acquisition card, DG- diffraction grating, FC – fiber coupler, FG- frame grabber, FI – Faraday isolator, GS – galvo scanners, L –lenses, MT – moving table, NDF – Neutral Density Filter, PC – polarization controller, SC – scanner controller, SLD – superluminescent diode

The system shown in Fig. 1 is similar to those described by others primarily due to the use of the same CCD line scan camera (12 bit, Atmel, 2048-pixels) that constrains the spectrometer design. The light in the spectrometer is collimated using a 100 mm focal length collimating objective (OZ optics) in front of the 1200 l/mm holographic transmitting diffraction grating (Wasatch Photonics). Two 300 mm focal length doublets are used to focus the light onto the CCD. This spectrometer allows maximum probing depth up to 2.7 mm in free space. The light source is a

Superluminescent diode (Superlum) with FWHM spectral range of 50 nm, centered at 841 nm and output power of 10 mW. The measured axial resolution of our system in free space, Δz , is 6 μm . A fiber-based Faraday isolator (FI) (OZ optics) protects the SLD against back reflections. The 80/20 fiber coupler (AC photonics) splits light into reference and sample arms. The moving table (MT) in the sample arm is used to match the path length in both interferometric arms. A Personal Computer drives the two galvo scanners (GS) for the X-Y scanning system (via scanner controller, SC). The clock signal from DAQ triggers both the driving signal for X-Y Scanners and starts CCD frame acquisition. The detected CCD signal is continuously streamed and overwritten to PC-RAM memory. When acquisition is complete, the last 200 B-frames are streamed to the PC hard drive. The C++ based acquisition software can work in two configurations allowing raw or real time displayed (Fourier transformed) image saving.

The current system speed limit is set by the CCD camera exposure time and its transfer rate to the PC. The shortest exposure time we used in this experiment is 50 μs , with 1000 A-scans per frame (5 ms/Frame). However the fastest frame acquisition achieved is 16 Fr/s for 50 and 9 Fr/s for 100 μs exposures. The power in the sample arm never exceeds 700 μW for all of the experiments which is within safety limits for safe use for our source.

The sample arm in our experimental system consists of a 10x microscope objective to collimate the light from a fiber and a 2x relay telescope using 30 and 60 mm focal length achromats to reduce the beam diameter entering the eye and to double the scanning angle of the X-Y scanners. This solution, similar to the one used in commercial OCT instruments (Zeiss Meditec), allows high scanning angle on the retina up to 40–50 deg (equivalent to 12-15mm).

To reduce eye and head motion of the subject, a dental impression mount on an x-y-z stage was used for all *in vivo* experiments. A fixation target has also been used to further reduce eye motion.

3. RESULTS

In order to test the performance of our FD-OCT system, we first recorded single A-scans for a mirror placed in the sample arm with known reflectivity of -50.2 dB (introduced by NDF). The results of this experiment for six different exposure times can be seen in the figure below:

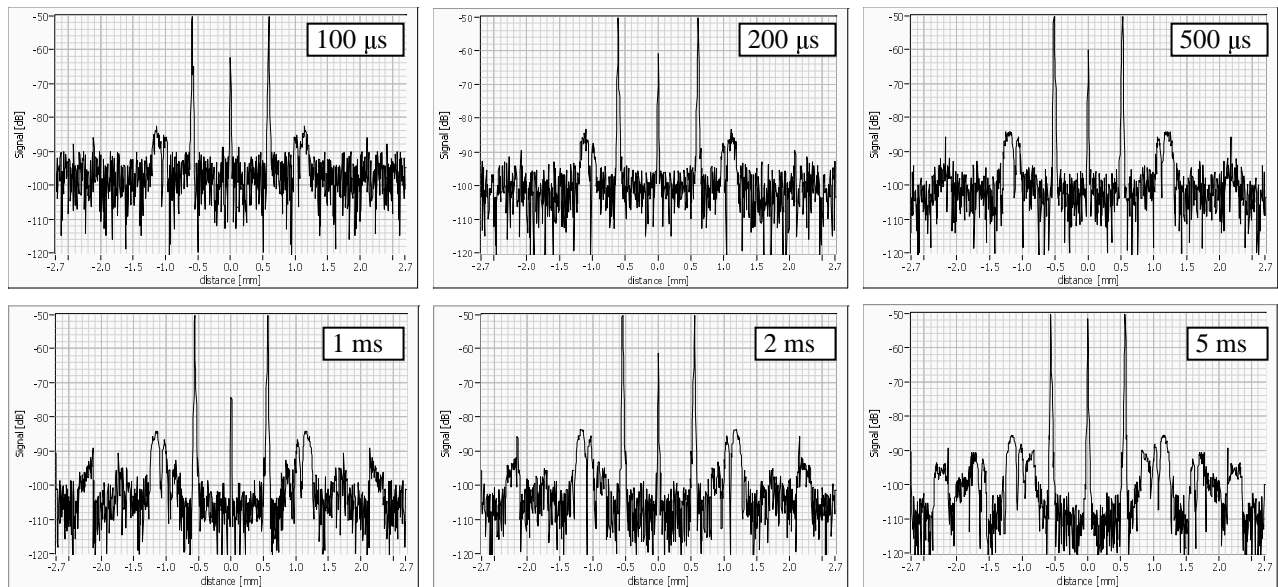


Figure 2. A-scans measured for a mirror placed at 500 μm OPD with NDF reducing its reflectivity to -50.02 dB for six different exposure times. Note that increasing exposure times decrease the noise floor to reveal the coherent noise.

As can be seen from Fig. 2 and in accordance with theoretical predictions from Eq. 4, increase of exposure time decreases the noise floor of the OCT signal. This does not, however, ensure improvement in image quality, the lower noise level unravels the coherent noise that lies about 35 dB below the signal. This can be explained by the term $O[I_s^2 / I_r^2]$ in Eq. 2. To optimize the performance of our system for each exposure time, the reference arm power has been

adjusted to not exceed $\frac{3}{4}$ of the CCD camera saturation level. This is $\sim 3,000$ Au for our 12-bit camera. Thus I_s representing the intensity from the sample arm as well as the coherence noise increases with exposure time. In this simulation we assumed a motion-free sample object.

Sensitivity was calculated using Equations 5 and 6 to compare our system performance with theoretical predictions. Fig. 3 presents the results of these studies demonstrating good agreement between experiment and theory.

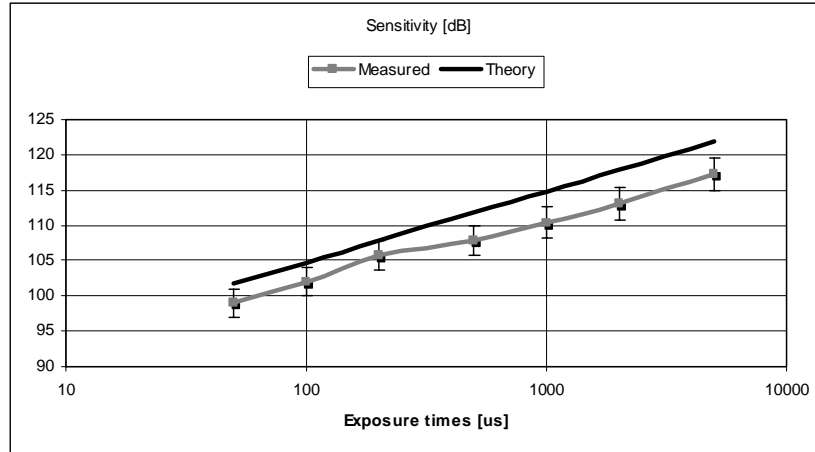


Figure 3. The experimental and theoretical sensitivity found for different exposure times.

It should be noted that for experimental sensitivity estimation we neglected the coherent noise so the noise standard deviation has been calculated on positions free of coherence noise. This approach may not, however, be correct for prediction of *in vivo* data quality.

Before showing the main results one comment about placing the reference mirror must be made. In our system only one spectrum is used to extract depth information. Thus, after the Fourier transform, two complex conjugated images are created. One of the simplest methods to overcome this problem is to place the investigated structure entirely on positive or negative optical path length difference (OPD) with respect to the reference mirror. The figure below provides an example of this situation.

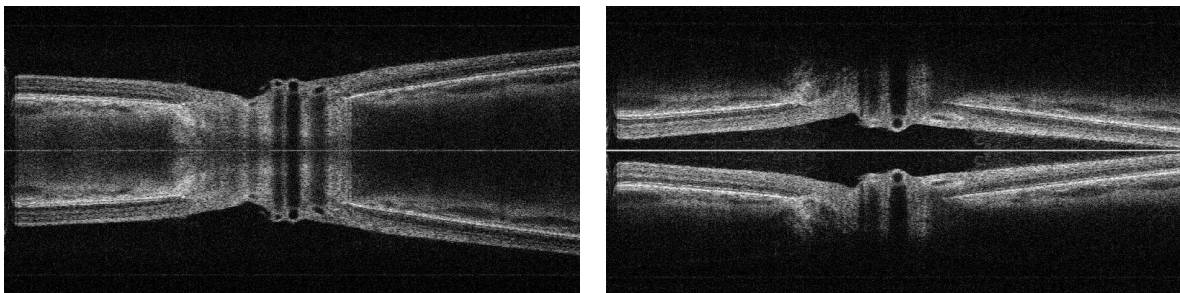


Figure 4. Full range image of FD-OCT *in vivo* Optical Nerve Head (ONH). Left image represents the case in which the whole retina occupies negative optical pathlength difference (OPD) to reference mirror position; right image represents positive OPD. Image size 8 x 4 mm (transversal x axial)

To reduce possible confusion when looking at two complex conjugated images, only the upper half of the image will be shown for negative OPD position of the retina and the lower half of the image for positive OPD retina placement.

To better test those two cases, both are used to image retinal structures for different exposure durations as shown in Fig. 5.

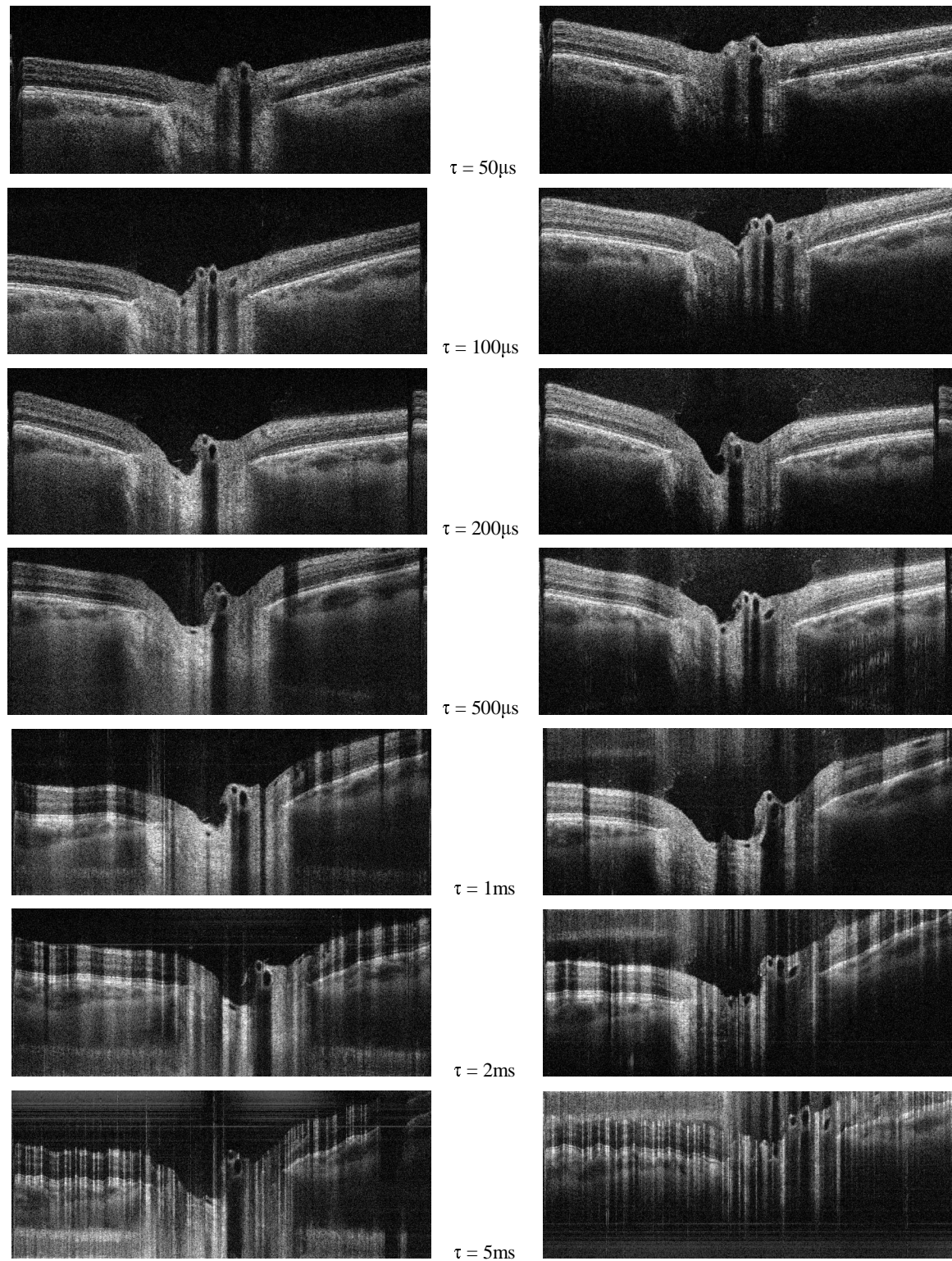


Figure 5. ONH *in vivo* retinal images acquired for different exposure times for negative (left column) and positive (right column) OPD position of the retina. All images are 8 mm x 1,6 mm (transversal x axial). Note the rather rapid image degradation for longer exposure times.

Figure 5 illustrates the dramatic reduction in image quality for exposures $\geq 500\mu\text{s}$. The wavy structures suggest that this may be due to axial motion of the eye. The transversal motion of the eye seems to manifest itself mainly as structure blur in the transverse direction.

One can also see that positive OPD images have higher noise levels (seen on all images in front of retinal structures), while for negative OPD it is covered by multiple scattering "tails" on the back of retinal structures. Thus these images look less noisy. It appears that placing a strongly scattering object close to zero OPD makes the coherent noise higher (as it is for positive OPD retina placement). The explanation can be found in Eq. 8, where signal drop off with path length difference may be observed. The figure below shows the measured signal degradation as a function of depth.

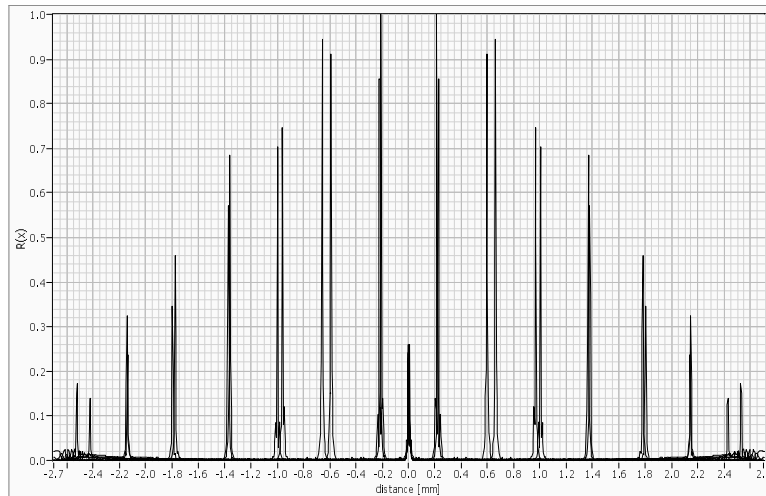


Figure 6. Measured signal reduction as a function of depth due to resolving power of spectrometer $R(x)$. Please note that $R(x)$ is plotted on a linear scale. This graph consists of 14 A-scans acquired for different samples superimposed one on another.

As can be seen from the Tomograms in Fig. 5, $R(z)$ can not only reduce the signal, but also the coherent noise level. Another interesting point is that some noise is not washed out by motion of the sample. Thus, they represent $O[I_s^2 / I_r^2]$ terms entirely created by internal reflections in the system.

4. CONCLUSIONS

We have shown that exposure time plays a critical role in image quality of Spectral OCT. The sensitivity values derived from theory as well as those measured for a nonmoving mirror placed in the sample arm does not correspond to retinal *in vivo* image quality for longer exposure times. Instead of seeing structures with better contrast, dramatic degradation is observed. To overcome this problem, the reduction of exposure time to $\leq 200\mu\text{s}$ per A-scan may be essential. If one would like to use longer exposure times for increasing system sensitivity, better head fixation may be helpful for achieving the desired performance. The use of pulsed light sources may help as well [15]. To reduce the influence of coherence artifacts the proper positioning of the retina may help. In our case, positioning the retina on a negative OPD reduced the influence of coherence noise.

ACKNOWLEDGEMENTS

We gratefully acknowledge the contributions of Donald T. Miller and Yan Zhang from the School of Optometry, Indiana University, Bloomington. This research was supported by the National Eye Institute (grant EY 014743).

REFERENCES

1. A.F. Fercher, C.K. Hitzenberger, G. Kamp, Y. Elzaiat, "Measurement of intraocular distances by backscattering spectral interferometry", *Opt. Commun.* **117**, 43-48 (1995)
2. G. Hausler, M.W. Lindner, "Coherence radar and spectral radar – new tools for dermatological diagnosis" *J.Biomed. Opt.* **3**, 21-31 (1998)
3. D. Huang, E.A. Swanson, C.P. Lin, J.S. Schuman, W.G. Stinson, W. Chang, M.R. Flotte, K. Gregory, C.A. Puliafito, "Optical Coherence Tomography", *Science* **254**, 1178-1181 (1991)
4. M. Wojtkowski, A. Kowalczyk, R. Leitgeb and A.F. Fercher "Full range complex spectral optical coherence tomography technique in eye imaging" *Opt. Lett.* **27**, 1415-1417 (2002)
5. M. Wojtkowski, T. Bajraszewski, P. Targowski and A. Kowalczyk "Real time in vivo imaging by high-speed spectral optical coherence tomography", *Opt. Lett.* **28**, 1745-1747 (2003)
6. N.A. Nassif, B. Cense, B.H. Park, M.C. Pierce, S.H. Yun, B.E. Bouma, G.J. Tearney, T.C. Chen, J.F. de Boer "In vivo high-resolution video-rate spectral-domain optical coherence tomography of the human retina and optic nerve", *Opt. Express* **12**, 367-376 (2004)
7. R.A. Leitgeb, W. Drexler, A. Unterhuber, B. Hermann, T. Bajraszewski, T. Le, A. Stingl, A.F. Fercher "Ultrahigh resolution Fourier domain optical coherence tomography" *Opt. Express*, **12**, 2156-2165 (2004)
8. M. Wojtkowski, V.J. Srinivasan, T.H. Ko, J.G. Fujimoto, A. Kowalczyk, J.S. Duker "Ultrahigh-resolution, high-speed, Fourier domain optical coherence tomography and methods for dispersion compensation" *Opt. Express*, **12**, 2404-2422 (2004)
9. B. Cense, N.A. Nassif, T.C. Chen, M.C. Pierce, S.-H. Yun, B.H. Park, B.E. Bouma, G.J. Tearney, J.F. de Boer "Ultrahigh-resolution high-speed retinal imaging using spectral-domain optical coherence tomography" *Opt. Express*, **12**, 2435-2447 (2004)
10. R. Leitgeb, C.K. Hitzenberger, A.F. Fercher, "Performance of fourier domain vs. Time domain optical coherence tomography", *Opt. Express* **11**, 889-894 (2003)
11. J.F. de Boer, B. Cense, B.H. Park, M.C. Pierce, G.J. Tearney, B.E. Bouma, "Signal to noise gain of spectral domain over time domain optical coherence tomography", *Opt. Lett.* **28**, 2067-2069 (2003)
12. M.A. Choma, M.V. Sarunic, C. Yang, J.A. Izatt "Sensitivity advantage of swept source and fourier domain optical coherence tomography", *Opt. Express* **11**, 2183-2189 (2003)
13. S.H. Yun, G.J. Tearney, J.F. de Boer, B.E. Bouma "Motion artifacts in optical coherence tomography with frequency-domain ranging" *Opt. Express* **12**, 2977-2998 (2004)
14. A.F. Fercher, W. Drexler, C.K. Hitzenberger and T. Lasser "Optical coherence tomography – principles and applications" *Rep. on Prog. in Physics* **66**, 239-303 (2003)
15. S.H. Yun, G.J. Tearney, J.F. de Boer, B.E. Bouma "Pulsed-source and swept-source spectral-domain optical coherence tomography with reduced motion artifacts" *Opt. Express* **12**, 5614-5624 (2004)